THE JOURNAL OF BIOLOGICAL CHEMISTRY
Vol. 279, No. 19, Issue of May 7, pp. 20137–20146, 2004

Printed in U.S.A.

Characterization of Na^+-permeable Cation Channels in LLC-PK1 Renal Epithelial Cells*

Received for publication, October 31, 2003, and in revised form, February 16, 2004
Published, JBC Papers in Press, February 24, 2004, DOI 10.1074/jbc.M311946200

Malay K. Raychowdhury‡§¶, Cristina Ibarra‖, Alicia Damiano‖**, George R. Jackson, Jr.‡, Peter R. Smith‡‡, Margaret McLaughlin‡, Adriana G. Prat‡‖, Dennis A. Ausiello‡§, Alan S. Lader‡§, and Horacio F. Cantiello‡§**§§**

*From the ‡Renal Unit, Massachusetts General Hospital East, Charlestown, Massachusetts 02129, the §Department of Medicine, Harvard Medical School, Boston, Massachusetts 02115, the ‖Departamento de Fisiología, Facultad de Medicina, Universidad de Buenos Aires, Buenos Aires 1121, Argentina, the **Laboratorio de Canales Iónicos, Química General e Inorgánica, Departamento de Fisicoquímica, Facultad de Farmacia y Bioquímica, Universidad de Buenos Aires, Buenos Aires 1113, Argentina, and the ‡‡Departments of Physiology and Biophysics, University of Alabama at Birmingham, Birmingham, Alabama 35294*

In this study, the presence of Na^+-permeable cation channels was determined and characterized in LLC-PK1 cells, a renal tubular epithelial cell line with proximal tubule characteristics derived from pig kidney. Patch-clamp analysis under cell-attached conditions indicated the presence of spontaneously active Na^+-permeable cation channels. The channels displayed nonrectifying single channel conductance of 11 pS, substates, and an ~3:1 Na^+/K^+ permeability-selectivity ratio. The Na^+-permeable cation channels were inhibited by pertussis toxin and reactivated by G protein agonists. Cation channel activity was observed in quiescent cell-attached patches after vasopressin stimulation. The addition of protein kinase A and ATP to excised patches also induced Na^+ channel activity. Spontaneous and vasopressin-induced Na^+ channel activity were inhibited by extracellular amiloride. To begin assessing potential molecular candidates for this cation channel, both reverse transcription-PCR and immunocytochemical analyses were conducted in LLC-PK1 cells. Expression of porcine orthologs of the αENaC and ApxL genes were found in LLC-PK1 cells. The expression of both gene products was confirmed by immunocytochemical analysis. Although αENaC labeling was mostly intracellular, ApxL labeled to both the apical membrane and cytoplasmic compartments of subconfluent LLC-PK1 cells. Vasopressin stimulation had no effect on αENaC immunolabeling but modified the cellular distribution of ApxL, consistent with an increased membrane-associated ApxL. The data indicate that proximal tubular LLC-PK1 renal epithelial cells express amiloride-sensitive, Na^+-permeable cation channels, which are regulated by the cAMP pathway, and G proteins. This channel activity may implicate previously reported epithelial channel proteins, although this will require further experimentation. The evidence provides new clues as to potentially relevant Na^+ transport mechanisms in the mammalian proximal nephron.

LLC-PK1 cells constitute an established cell line derived from normal pig kidney displaying several characteristics of the proximal tubule (1–3). Na^+ transport by LLC-PK1 cells has been associated with coupled mechanisms, including amino acids (2), glucose (4), and inorganic phosphate co-transport (5). Na^+ exchange with hydrogen ions mediated by the Na^+/H^+ exchanger has also been described (6). Radioisotopic Na^+ fluxes in LLC-PK1 monolayers provided the first evidence for the presence of an amiloride-sensitive electrodiffusional Na^+ transport pathway (7) with several similarities to that observed at the apical membrane of tight epithelia (8). At least one other study determined that electrically sensitive, but pH-insensitive Na^+ transport in LLC-PK1 cells displays pharmacological characteristics different from those expected from ENaC channels (9). A preliminary patch-clamp study suggested, however, the presence of amiloride-sensitive, Na^+ channel activity in LLC-PK1 cells (10). In the present report, patch-clamping techniques and membrane reconstitution assays were applied to subconfluent LLC-PK1 cells, and membranes, respectively, to determine whether this renal tubular epithelial cell model indeed expresses Na^+-permeable cation channels. The data indicate the presence of amiloride-sensitive Na^+-permeable, 11-pS cation channels, whose activity is modulated by the cAMP pathway and G proteins. The presence of αENaC and ApxL was determined by RT-PCR.[1] The expression of the gene products was also confirmed in the LLC-PK1 cells by immunocytochemical and Western blot analyses. The present data suggest that the mammalian equivalent of Apx, ApxL, and/or αENaC may be components of a Na^+ channel complex involved in Na^+ reabsorption in the mammalian proximal nephron.

EXPERIMENTAL PROCEDURES

Cell Cultures—LLC-PK1 cells (ATCC CRL1392) were grown and kept in a Dulbecco's modified Eagle's medium supplemented with 10% fetal bovine serum and 1% L-glutamine as previously described (6, 7). The cells were grown on glass coverslips until partially confluent and kept in humidified atmosphere at 37 °C in 5% CO_2 gassed air. The 293 human embryonic kidney cells (ATCC CRL1573) were also grown and kept in humidified atmosphere at 37 °C in 5% CO_2 gassed air. A6 renal epithelial cells derived from *Xenopus laevis* (ATCC CCL102) were grown as previously described. Briefly, the cells were kept in a Coon's modification of Ham's F-12 and Liebovitz's F15 media modified to

* This work was supported in part by National Institutes of Health Grant DK48040 (to H. F. C.). The costs of publication of this article were defrayed in part by the payment of page charges. This article must therefore be hereby marked "*advertisement*" in accordance with 18 U.S.C. Section 1734 solely to indicate this fact.

¶ Supported by National Institutes of Health Training Grant T32DK07540C15.

§§ To whom correspondence should be addressed: Renal Unit, Massachusetts General Hospital East, 149 13th St., Charlestown, MA 02129. Tel.: 617-726-5640; Fax: 617-726-5669; E-mail: cantiello@helix.mgh.harvard.edu.

[1] The abbreviations used are: RT, reverse transcription; MOPS, 4-morpholinepropanesulfonic acid; MES, 4-morpholineethanesulfonic acid; PKA, cAMP-dependent protein kinase; PBS, phosphate-buffered saline; AVP, arginine vasopressin; PTX, pertussis toxin; GTPγS, guanosine 5′-*O*-(3-thiotriphosphate); pS, picosiemens.

contain 105 mM NaCl and 25 mM $NaHCO_3$. This mixture was supplemented with 10% fetal bovine serum (Invitrogen). A6 cells were also grown and kept in humidified atmosphere at 27 °C in 5% CO_2 gassed air.

Single Channel Studies—Cell-attached and excised, inside-out patch-clamp experiments were carried out as previously described (11, 12). Currents and command voltages were obtained and driven with a PC-501 patch-clamp amplifier using a 10 gigaohm head stage (Warner Instruments, Hamden, CT). The signals were filtered at 1 kHz with an eight-pole Bessel filter (Frequency Devices, Haverhill, MA). The data were stored in a hard disk of a personal computer and analyzed with PClamp 6.0.3 (Axon Instruments, Burlingame, CA). The Data were further filtered at 200 Hz for display purposes. For excised patches, upward and downward deflections indicated the channel open state at positive and negative holding potentials, respectively. Holding potentials between ± 100 mV refer to the patch-pipette. The patch-pipette and bathing solution was 135 mM NaCl, 5.0 mM KCl, 0.8 mM $MgSO_4$, 1.2 mM $CaCl_2$, and 10 mM Hepes, pH 7.4. When indicated, Na^+ was replaced by an equimolar concentration of K^+, and Cl was replaced by aspartate. All other solutes remained the same.

Ion Channel Reconstitution—Lipid bilayers were formed with a mixture of synthetic phospholipids (Avanti Polar Lipids, Birmingham, AL) in *n*-decane as recently reported (13). The lipid mixture was made of 1-palmitoyl-2-oleoyl phosphatidylcholine and phosphatidylethanolamine in a 7:3 ratio. The lipid solution (~20–25 mg/ml) in *n*-decane was spread with a glass rod over the 250-μm-diameter aperture of a polystyrene cuvette (CP13–150) of a bilayer chamber (model BCH-13; Warner Instruments Corp.). Both sides of the lipid bilayer were bathed with a solution containing MOPS-NaOH, 10 mM, and MES-NaOH, 10 mM, pH 7.40, and 10–15 μM Ca^{2+}. The final Na^+ concentration in the solution was ~15 mM. NaCl was further added to the *cis*-compartment, from which membrane vesicles were added, such that final concentrations of 150 Na^+ and 135 Cl^- were achieved in this side of the chamber. The experiments were also conducted with Na^+ aspartate, with a similar outcome. The electrical signals were recorded using a current-to-voltage converter with a 10 Gohm feedback resistor, as per single channel recordings (patch-clamp). Output (voltage) signals were low pass filtered at 700 Hz with an eight pole, Bessel type filter (Frequency Devices, Haverhill, MA). Single channel current tracings were further filtered (see "Results") for display purposes only. Unless otherwise stated, pCLAMP version 5.5.1 (Axon Instruments, Foster City, CA) was used for data analysis, and Sigmaplot Version 2.0 (Jandel Scientific, Corte Madera, CA) was used for statistical analysis and graphics.

Reconstituted Channel Activation and Inhibition and Calculations of Channel Open Probability—Channels reconstituted from LLC-PK1 membranes by the lipid bilayer system were activated by addition of PKA (10 μg/ml) and MgATP (1 mM). This was conducted by one of two methods. In some experiments, channel activity was determined under control conditions, prior to the PKA activation procedure. Once cation-selective channel activity was confirmed, PKA and ATP addition was conducted to the *cis*-side of the chamber (see Fig. 2*a*, *inset*). Only channels whose activity was increased (or activated by) PKA addition to this side of the chamber were further studied. This was done to ensure that only channels incorporated in the "correct" orientation for activation/inhibition were studied. PKA-activated channels were active for longer than 30 min, and run-down was never observed. On the contrary, some experiments were unfinished because high channel activity tended to break the reconstituted membrane. Once channel activity was confirmed and channel levels were identified on the oscilloscope, the addition of amiloride was conducted to the *trans*-side of the chamber (see Fig. 2*a*, *inset*). In most cases where identified channel activity was observed (up to six channel levels), the open probability (p_o) was calculated as previously reported (36). Briefly, the p_o of the channel was obtained from the following equation,

$$\sum_{i=1}^{n=N} \frac{n(t_o)}{N} \qquad \text{(Eq. 1)}$$

where t_o equals the total time at a given level (n) from a total channel number (N). The p_o was confirmed by approximation (10%) to the value $p'_o = 1 - (t_c)1/N$, where p'_o is the p_o as calculated from the inverse of the total closed time (t_c), and N reflects the total channel number, as before. For multichannel records, the mean membrane currents from various reconstituted membranes were averaged and compared as indicated below.

Immunocytochemistry—Immunocytochemical analysis of αENaC and ApxL was performed as previously described (12). Briefly, immunocytochemistry analysis was conducted as follows. LLC-PK1 cells were fixed in 5% paraformaldehyde in 0.05% phosphate buffer for 20 min at room temperature. A goat anti-rabbit secondary Alexa fluor 594 (Molecular Probes) antibody was used at 1:800. Conversely, LLC-PK1 cells were grown on glass coverslips for 2–4 days (80% confluent). The cells were fixed in 5% paraformaldehyde in 0.05% phosphate buffer for 20 min at room temperature. Conversely, the cells were fixed with 4% paraformaldehyde, 0.1% glutaraldehyde, and 5% sucrose in phosphate-buffered saline (PBS) for 40 min at room temperature, followed by cell permeabilization with 0.1% Triton X-100 for 5 min. After incubation with PBS containing 1% bovine serum albumin to block nonspecific binding (10 min), coverslips were incubated for 1 h with the primary antibody diluted 1:100 in PBS. After extensive washing, either goat anti-rabbit IgG coupled to CY3 (indocarbocyanine; Jackson ImmunoResearch Laboratories, West Grove, PA) was applied (1:400) or a goat anti-rabbit secondary Alexa fluor 594 (Molecular Probes, 1:800). LLC-PK1 cells were counterstained with Evans Blue (1:800) to assess the cellular morphology along with channel protein staining. After further washing in PBS, the coverslips were mounted in Vectashield antifading medium (Vector Labs, Burlingame, CA) diluted 1:1 in 0.3 M Tris base, pH 8.9, sealed, and examined with a Nikon FXA fluorescence microscope. The images were captured using an Optronics 3-bit CCD color camera (Optronics Engineering, Goleta, CA), and IP Lab Spectrum (Scanalytics, Vienna, VA) acquisition and analysis software running on a Power PC 8500 (Apple Computer, Cupertino, CA). The images were imported as TIFF files into Adobe Photoshop 4.0.1 for size reduction and editing.

Membrane Preparations and Western Blot Analysis—The cell membranes from LLC-PK1 cells were obtained according to procedures previously described (12). Briefly, subconfluent cultures of LLC-PK1 cells were scraped and centrifuged at 3,000 rpm for 10 min at 4 °C. After suspension in 1 ml of buffer containing 250 mM sucrose, 10 mM Tris-base, pH 7.6, 50 mM NaCl, and 1× protease inhibitor mixture, the cell pellet was sonicated twice for 10 s in a sonicator (Ultrasonic Processor, model XL2020; Misonix Inc.). Sonication was repeated after the addition of protease inhibitor buffer (9 ml). Supernatant obtained after centrifugation for 10 min at 3,000 rpm was further ultracentrifuged at 25,000 rpm for 1h at 4 °C in an L8–80 M Ultracentrifuge (Beckman, Palo Alto, CA), using a swing rotor SW41 Ti. The pellet was suspended in 200 μl of protease-inhibitor buffer and used for both immunoblot analysis and channel reconstitution (see above). The membrane preparation was separated by 4–12% SDS-PAGE and electroblotted into a polyvinylidene difluoride membrane. The blots were immunoblotted with anti-αENaC and anti-Apx antibodies separately (both antibodies were a kind gift of Dr. Tom Kleyman).

Antibodies—The primary anti-Apx antibody was a rabbit polyclonal serum raised against an Apx fusion protein containing the Apx COOH terminus (amino acids 1194–1395) (12). Anti-αENaC antibodies were from CalBiochem (San Diego, CA). Primary antibodies were used at a 1:100 dilution as previously described (12). Rabbit, anti-human antibodies were raised against an immunogenic synthetic peptide (LMKGNKREEQGLGPEPAAQQPT(C)) corresponding to amino acid residues 20–42 of the human αENaC. Otherwise, rabbit anti-rat antibodies were raised against an immunogenic peptide corresponding to residues 44–57 (GLGKGDKREEQGLG) within the NH_2-terminal intracellular domain of rat αENaC (14).

Total RNA Isolation—Total RNA was isolated from LLC-PK1, 293, and A6 cultured cells using a TRIzoL RNA extraction kit (Invitrogen) following the manufacturers recommended procedures. The isolated RNA was quantified by absorbance at 260 nm and stored at −80 °C until further use.

RT-PCR Analysis—The RT-PCR assay was performed in two steps using ThermoScript RT-PCR System (Invitrogen). In the first step, total RNA (nearly 2 μg) was incubated for 60 min at 55 °C with reverse primers (0.2 μg each) for first strand cDNA synthesis. For ApxL, a second step was conducted, including 35 PCR cycles at 96 °C (1 min). This was followed by 55 °C (1 min) and 72 °C (3 min), and a final extension for 10 min at 72 °C. For αENaC, an additional hot start step was performed 96 °C (6 min). Forward and reverse primers (0.5 μg each) for ApxL were 5′-TGGCCACCAATTCTACCTA-3′ (residues 4265–4283) and 5′-CCGACTTCATCTTCACGAAG-3′ (residues 4840–4821), respectively, from the COOH terminus of human ApxL sequence (15) and were used to amplify a 575-bp band. For αENaC, forward and reverse primers (0.5 μg each) 5′-CTGTCCGTGGTGGAGATGGCT-3′ (residues 2341–2361) and 5′-CCCTCGGCCTGGGGACCAGTA-3′ (residues 2445–2425), respectively, in the conserved region of bovine αENaC (16) were used to amplify a 105-bp band. RT-PCR products were separated on either 1.5 or 3% agarose gels. The amplified bands were

subjected to automated DNA sequence analysis at the Massachusetts General Hospital DNA Sequencing Center.

Other Reagents—Both lysine vasopressin and arginine vasopressin (AVP; Sigma), were kept in 0.1 mM stock solutions in distilled water and used at 10 nM and 10 μM final concentration, respectively. The catalytic subunit of the PKA was obtained from Sigma and used at a final concentration of 10 μg/ml. MgATP (Sigma) was used at a final concentration of 1 mM. Pertussis toxin (PTX) was obtained from Peninsula Labs. (Belmont, CA) and stored at −20 °C. The toxin was activated in a stock solution containing 1000 mM NaCl, 20 mM Na_2HPO_4, pH 7.0. The solution also contained 10 mM dithiothreitol and 1 mM NAD^+ as previously described (17). Activated PTX (3 μl) was added to the patch-clamp chamber (0.3 ml). The final concentration was ~100 ng/ml. GTPγS (Sigma) was kept in a stock solution containing 10 mM Hepes, pH 7.6, at 0 °C. The final nucleotide concentration was 100 μM.

Calculation of Na^+/K^+ Permeability-Selectivity Ratio and Amiloride Inhibitory Constant—The Goldman-Hodgkin-Katz equation was used to calculate the permeability-selectivity ratio P_{Na}/P_K, using the following equation,

$$P_{Na}/P_K = z_2{}^K \times K_o \times \exp(\alpha z_K E_r) \times (1 - \exp(\alpha z_{Na} E_r)) /(z^2{}_{Na} \times Na_i \times (1 - \exp(\alpha z_K E_r))) \quad \text{(Eq. 2)}$$

where $\alpha = F/RT$, z_{Na} is the valence of Na^+, and z_K is the valence of K^+. The subscripts i and o represent the intracellular and extracellular compartments, respectively. E_r is the reversal potential, and all the other symbols represent their usual meaning.

The inhibitory constant for amiloride (K_i) on channel activity from reconstituted LLC-PK1 plasma membranes was calculated as previously described (12). Briefly, the mean currents from reconstituted plasma membranes were obtained in the absence and presence of various concentrations of amiloride ([Amil]). The decrease in membrane current was calculated as percentage of control current ($100 \times I_{Amil}/I_{Ctr}$) and fitted to the equation $100 - 100 \times ([Amil]/[Amil] + K_i)$, representing the fractional decrease in mean current as a function of the amiloride concentration. Whenever indicated, this equation was expanded to include two independent amiloride-binding sites.

RESULTS

Functional Characterization of Na^+-permeable Channels in LLC-PK1 Cells—Single channel currents were obtained to assess the functional presence of Na^+-permeable cation channels in LLC-PK1 renal epithelial cells. Under cell-attached conditions, spontaneous Na^+ channel activity was observed in 17 of 58 experiments (29.3%). After excision, using a symmetrical Cl-free Na^+ solution, spontaneous Na^+ channels were observed in 65 of 148 experiments (44%; Fig. 1*a*). The single channel conductance in 135 mM Na^+ was 11.1 ± 1.20 pS (n = 9; Fig. 1*b*) and did not rectify between −100 mV and +100 mV. However, under asymmetrical Na^+ *versus* K^+ conditions with K^+ in the bath, the single channel currents rectified, and the reversal potential shifted from zero to −36 ± 4.5 mV, indicating a higher Na^+ over K^+ permeability-selectivity ratio (Fig. 1*b*). Under these conditions, a Na^+/K^+ permeability-selectivity ratio (P_{Na}/P_K) of ~3:1 was obtained by fitting the experimental data with the Goldman-Hodgkin-Katz equation (Fig. 1*b*). Na^+ channel activity in asymmetrical Na^+/K^+ also displayed frequent subconductance states (Fig. 1*c*). Diffusion of amiloride (100 μM) from the patch pipette (see Ref. 11 for technical details) showed a slow decrease and complete inhibition of the Na^+ currents in cell-attached and excised inside-out patches (Fig. 1*d*). The spontaneous Na^+ channel activity of LLC-PK1 cells was similar to that previously reported in A6 epithelial cells (17–19).

Ion Channel Reconstitution and Affinity for Amiloride—To further assess the amiloride sensitivity of the Na^+-permeable channels in LLC-PK1 cells, the plasma membranes from these cells were reconstituted into lipid bilayers to assess for cation-selective ion channel activity (Fig. 2). Channel activity was observed in 11 of 14 experiments in either asymmetrical NaCl (150/15 mM; Fig. 2*a*) or Na^+-aspartate. Spontaneous Na^+-permeable channel activity increased by 191% (n = 25, $p < 0.005$; Fig. 2) (or otherwise activated) by the addition of PKA (10 μg/ml) and MgATP (1 mM) to the *cis*-side but not the *trans*-side of the reconstituted membranes (Fig. 2*a*, *inset*). Reconstituted channels had a single channel conductance of 15.6 pS (n = 3) and a lower subconductance state (Fig. 2*b*). The PKA-activated Na^+-permeable channel activity decreased by 80% after the addition of amiloride (1 μM; Fig. 2*c*). To assess the affinity for the amiloride inhibition of the Na^+ channel activity in LLC-PK1 cell membranes, various concentrations of the drug were added to the *trans*-side of the chamber (Fig. 2*d*). The addition of 50 nM amiloride was sufficient to decrease the open probability of the channel by 30% (n = 3) as calculated under "Experimental Procedures." The data were obtained from open and closed times at any given current level, from best fittings of open and closed dwell histograms (Fig. 2*e*). The mean currents were also obtained before and after the addition of increasing concentrations of the drug in multichannel records. The fractional data (as percentage) were fitted to an equation rendering a best fit of K_i = 80.4 nM (n = 7; Fig. 2*f*) for a single amiloride binding site. The data were also fitted with two putative binding sites (data not shown), which was not statistically different from the single site. The data would suggest the possibility that either one or two K_i, namely K_{i1} = 74.2 nM and K_{i2} = 3.99 μM, respectively, may be involved in binding and inhibiting 94 and 6% of the total current, respectively.

Regulation of Na^+-permeable Channels in LLC-PK1 Cells—To assess whether vasopressin, known to activate the cAMP pathway in LLC-PK1 cells, regulates the Na^+-permeable channel activity in these cells (20, 21), AVP was added to cell-attached patches. The addition of either lysine vasopressin (10 nM) or AVP (10 μM) readily induced Na^+ channel activity on otherwise quiescent cell-attached patches from LLC-PK1 cells in 5 of 7 experiments (71%; Fig. 3*a*). The current-voltage relationship of the AVP-induced Na^+ channel activity was highly similar to that obtained for AVP-stimulated Na^+ channels of A6 cells (Fig. 3*b*) (19). To further assess the effect of the cAMP pathway on Na^+ channel activity of LLC-PK1 cells, PKA (10 μg/ml) was also tested on quiescent excised inside-out patches (Fig. 3*c*). The addition of PKA plus ATP (1 mM) induced single channel currents (Fig. 3*c*, *inset*). Single channel open states often showed a smaller subconductance indicated by the open state noise distribution (Fig. 3*c*, *histogram*). Single channel currents of both AVP stimulation and/or PKA addition showed identical single channel conductance (Fig. 3*d*): 8.29 ± 3.05 pS (n = 13) *versus* 8.11 ± 0.98 pS (n = 17). These values were slightly lower but not statistically different from that obtained under spontaneous conditions ($p < 0.2$). The single channel currents observed after AVP activation, however, showed higher dispersion than that after PKA stimulation, suggesting a difference in the substate residence times between the two activating methods. To test whether Na^+ channel activity of LLC-PK1 cells is regulated by G proteins, the effect of PTX (100 ng/ml) was assessed in excised in inside-out patches (n = 4). Activated PTX completely blocked the spontaneous Na^+ channel activity (Fig. 3*e*, *middle tracing*), which reversed after the addition of the nonhydrolyzable GTP analog, GTPγS (1 mM; Fig. 3*e*, *bottom tracing*). This is consistent with the inhibitory effect of PTX on the 9 pS (17) but not the lower conductance (22) Na^+ channels present in A6 renal epithelial cells.

RT-PCR Detection of αENaC and ApxL in LLC-PK1 Cells—To begin an assessment of potentially relevant proteins associated with the Na^+ channel activity in LLC-PK1 cells, the presence of porcine orthologs of both ENaC and Apx was explored. The expression of αENaC in LLC-PK1 cells was conducted with primers specific for the bovine αENaC subunit as previously reported (16). An expected band of 105 bp was ob-

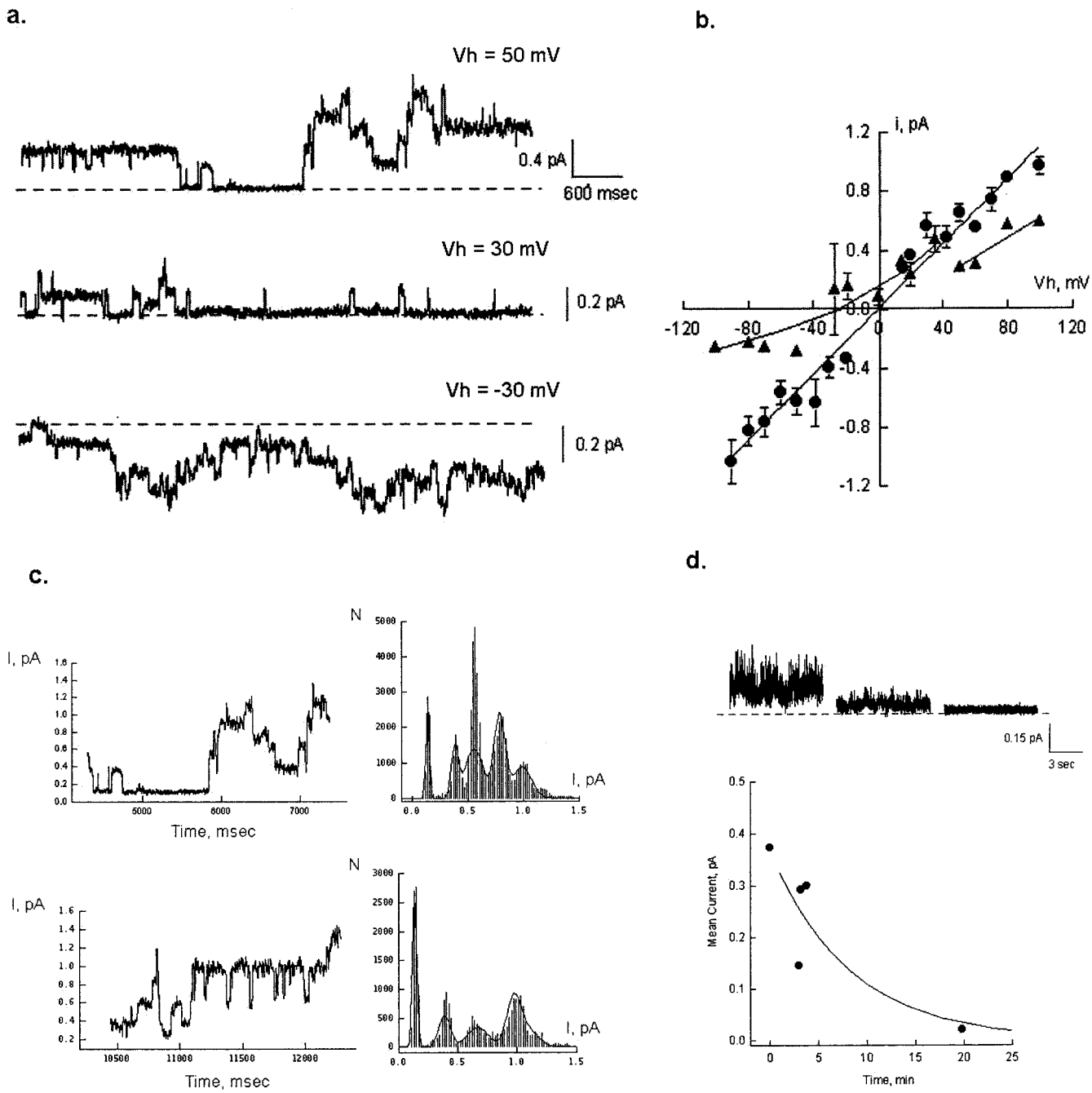

FIG. 1. **Na^+channel activity of LLC-PK1 cells.** *a*, excised, inside-out patches from LLC-PK1 cells displayed spontaneous Na^+ channel activity. V_h indicates the holding potential applied to the pipette. *b*, current-voltage relationship of spontaneous Na^+ channel activity of LLC-PK1 cells obtained in symmetrical Na^+ (135 mM NaCl or Na^+-aspartate, *circles*) or asymmetrical Na^+ *versus* K^+ conditions (135 mM NaCl *versus* KCl, *triangles*). The *solid lines* indicate linear and Goldman-Hodgkin-Katz fittings of data under symmetrical Na^+ and Na^+/K^+ conditions, respectively. The data are the means ± S.E. obtained from 17 and 7 independent experiments for symmetrical and asymmetrical conditions, respectively. *c*, expanded tracings in symmetrical Na^+ indicate the presence of multiple single channel levels of identical conductance (*top panels*) and frequent currents of higher subconductance level (*bottom panels*). *d*, amiloride blockage of Na^+ channel currents. *Top panel*, cell attached patches with multiple spontaneous channel activity were inhibited by diffusion of amiloride (100 μM) from the patch pipette as previously described (11). Time-dependent decay in the mean patch current is shown in the *bottom panel*. The data are representative of three experiments.

served after one RT-PCR cycle, consistent with the presence of this ENaC subunit (Fig. 4*a*). The αENaC mRNA of LLC-PK1 cells was highly homologous (>90%) to the human αENaC subunit. The mammalian isoform of the Apx gene (ApxL) was also examined in LLC-PK1 cells by RT-PCR with specific primers from the COOH-terminal end of the human ApxL sequence (15). PCR products of appropriate mobility were determined on a 1.5% agarose gel using A6 cell mRNA as a positive control (Fig. 4*b*). The expected band of 575 bp for the ApxL primers was amplified from the LLC-PK1 material. The primers were also able to detect amphibian Apx (A6 cell). The LLC-PK1 product was more than 90% homologous to human ApxL (Fig. 4*b*), suggesting the presence of a porcine ortholog of this protein in the pig kidney cells.

Immunolocalization of αENaC in LLC-PK1 Cells—The presence of αENaC in LLC-PK1 cells was also determined by immunolocalization with anti-αENaC antibodies. Despite strong nonspecific immunodetection in the presence of antigenic peptide (Fig. 5*b*), αENaC labeling was observed in control LLC-PK1 cells (Fig. 5*a*), in particular, at the intracellular level.

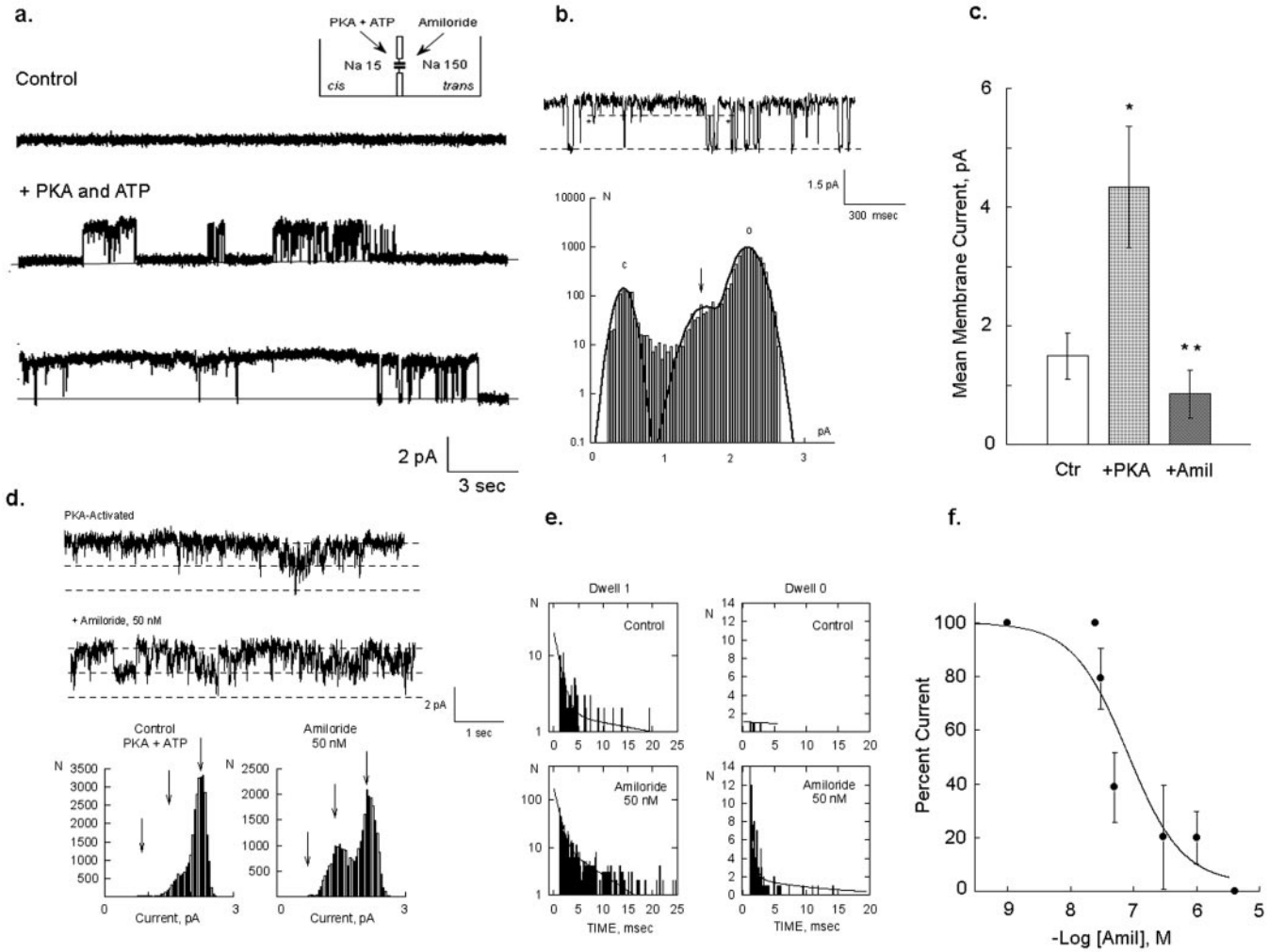

FIG. 2. **Channel reconstitution of LLC-PK1 membranes.** *a*, membrane-enriched preparations from LLC-PK1 cells were reconstituted into lipid bilayers using asymmetrical 150 mM NaCl. Channel activity was either induced and/or increased by the addition of PKA (10 μg/ml) plus MgATP (1 mM) to the *cis*-side of the reconstitution chamber (*inset*). The *inset* shows a schematic diagram of the reconstitution chamber where PKA activation took place by the addition to the *cis*-side of the chamber, and all of the additions of the inhibitor amiloride were conducted to the *trans*-side of the chamber. This ensured that only channels in a given orientation were activated and subsequently inhibited by amiloride. *b*, expanded recording to indicate the presence of subconductance states. *c*, channel activity was activated by PKA and ATP (*, $p < 0.01$, $n = 17$) was also inhibited by amiloride (1 μM, **, $p < 0.05$, $n = 4$) added to the *trans*-side of the chamber. *d*, PKA-activated channels (*top tracing*) were inhibited by the addition of amiloride to the *trans*-side of the reconstitution chamber. In this representative case ($n = 3$), showing two channel levels, the addition of 50 nM amiloride did not modify the amplitude of the channel (*bottom all-point histograms*). Instead, there were more frequent closings as shown in *e*. *e*, dwell histograms indicate that no changes in the open state (*left panels*) but increased, longer closed states (*right panels*) were induced by as little as 50 nM amiloride. This is also reflected in the one channel level currents in the all-point histograms (*d*, *bottom panels*). The calculated open probability (36) decreased by 29% in this example (see "Experimental Procedures" for details). *f*, channels were inhibited by increasing concentrations of amiloride to the *trans*-side of the reconstitution chamber. As in *d*, PKA-activated channel activity was obtained before and after the addition of increasing concentrations of amiloride ([Amil]). The data were expressed as percentages of mean membrane currents *versus* [Amil] and fitted (solid line) to indicate a single inhibitory site with $K_i = 80$ nM ($n = 7$).

Highly transporting cells (domes; Fig. 5*c*) showed somewhat stronger αENaC expression. However, no redistribution of αENaC labeling was detected after activation with either lysine vasopressin (10 nM) or AVP (10 μM) for 5 to 15 min (Fig. 5*d*).

Immunolocalization of ApxL in LLC-PK1 Cells—The presence of ApxL in LLC-PK1 cells was determined by immunolocalization with an anti-Apx-specific antibody. This antibody was previously used to detect Apx expression in A6 cells (23) and Apx-transfected human melanoma cells (12). Apx labeling was observed in control LLC-PK1 cells, in particular, at the subapical level (Fig. 6*A*). Labeling was performed with anti-Apx antibody (FITC, *green labeling*) and Evans Blue (*red*) to stain for cellular morphology and thus assess cell integrity. In most cases, Apx labeling was observed at the periphery of subconfluent LLC-PK1 cell islands (Fig. 6*A*), suggesting that cell growth and spreading of LLC-PK1 cells may affect ApxL expression. AVP treatment (10 μM; Fig. 6) of LLC-PK1 cells for 15 min prior to Apx labeling displayed an increased membrane staining for Apx. AVP treatment showed more Apx-labeled cells (Fig. 6*B*). Thus, AVP not only increased Apx labeling but also induced a redistribution of the protein in LLC-PK1 cells.

Apx(L) and αENaC Western Blot Analysis—The possible interaction between Apx(L) and αENaC is an issue that will further clarify the molecular structure and functional dynamics of the Na^+-permeable cation channels of LLC-PK1 cells. To assess whether Apx(L) peptides and ENaC subunits may interact with each other, Western blot analysis of plasma membranes was conducted with antibodies used for the immunolocalization studies. The membranes were prepared as for the channel reconstitution assays. The membranes were separated into aliquots and subjected to gel electrophoresis, blotted, and labeled with Apx and αENaC antibodies in the absence or presence of competing peptides. Several peptides were ob-

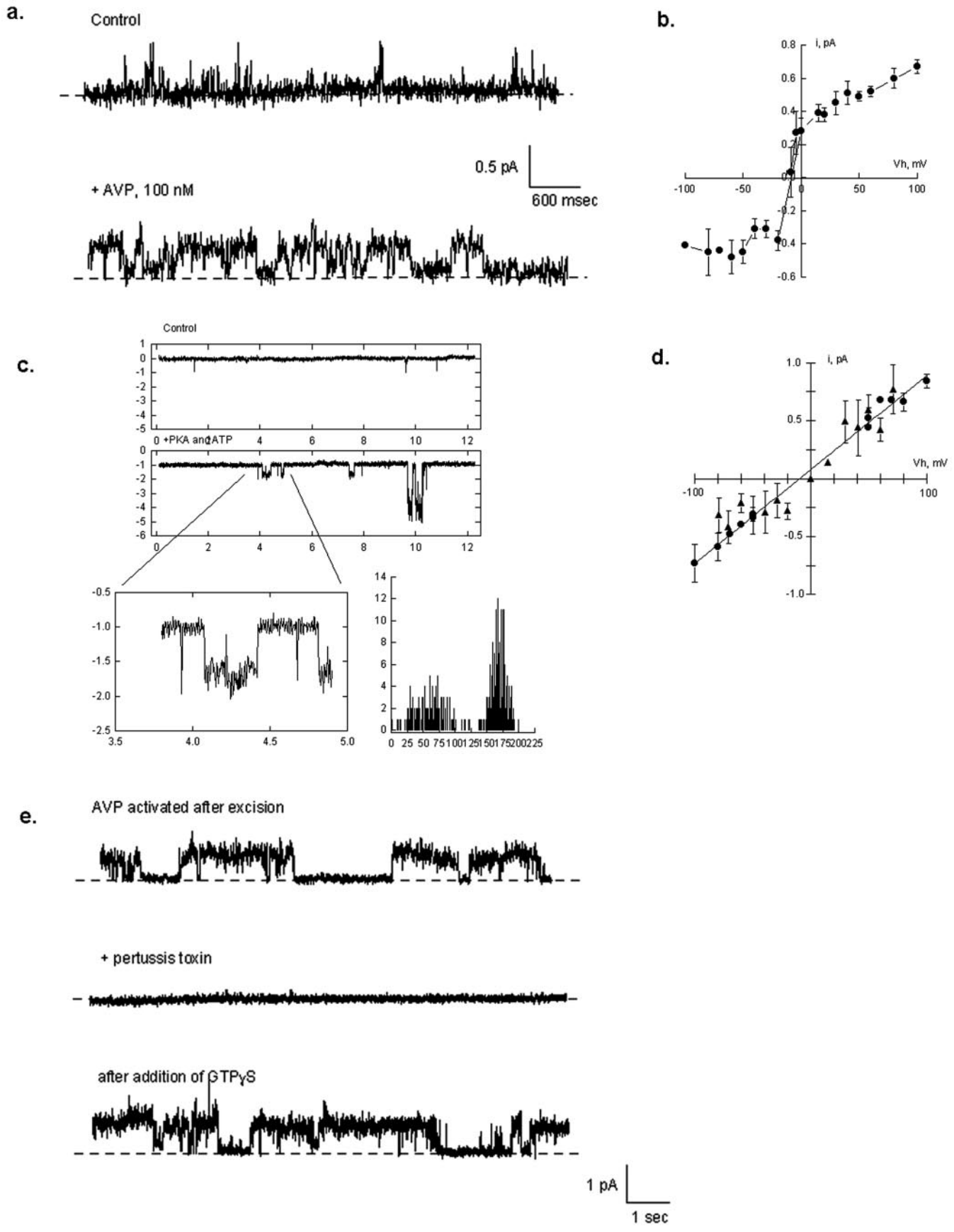

FIG. 3. **Regulation of Na^+ channel activity in LLC-PK1 cells.** *a*, addition of AVP (100 nM) to quiescent cell-attached patches (*top tracing*) induced Na^+-selective single channel activity (*bottom tracing*). *b*, single channel current-voltage relationship of LLC-PK1 Na^+ channels under cell-attached conditions. The data are the means ± S.E. obtained from nine experiments. *c*, addition of PKA (10 μg/ml) plus ATP (1 mM) to quiescent excised inside-out patches (*top tracing*) induced Na^+-selective single channel activity (*bottom tracing*). The data are representative of 10 experiments obtained in symmetrical Na^+. Expanded tracing indicates the single channel current (*left bottom panel*), and all-point histogram

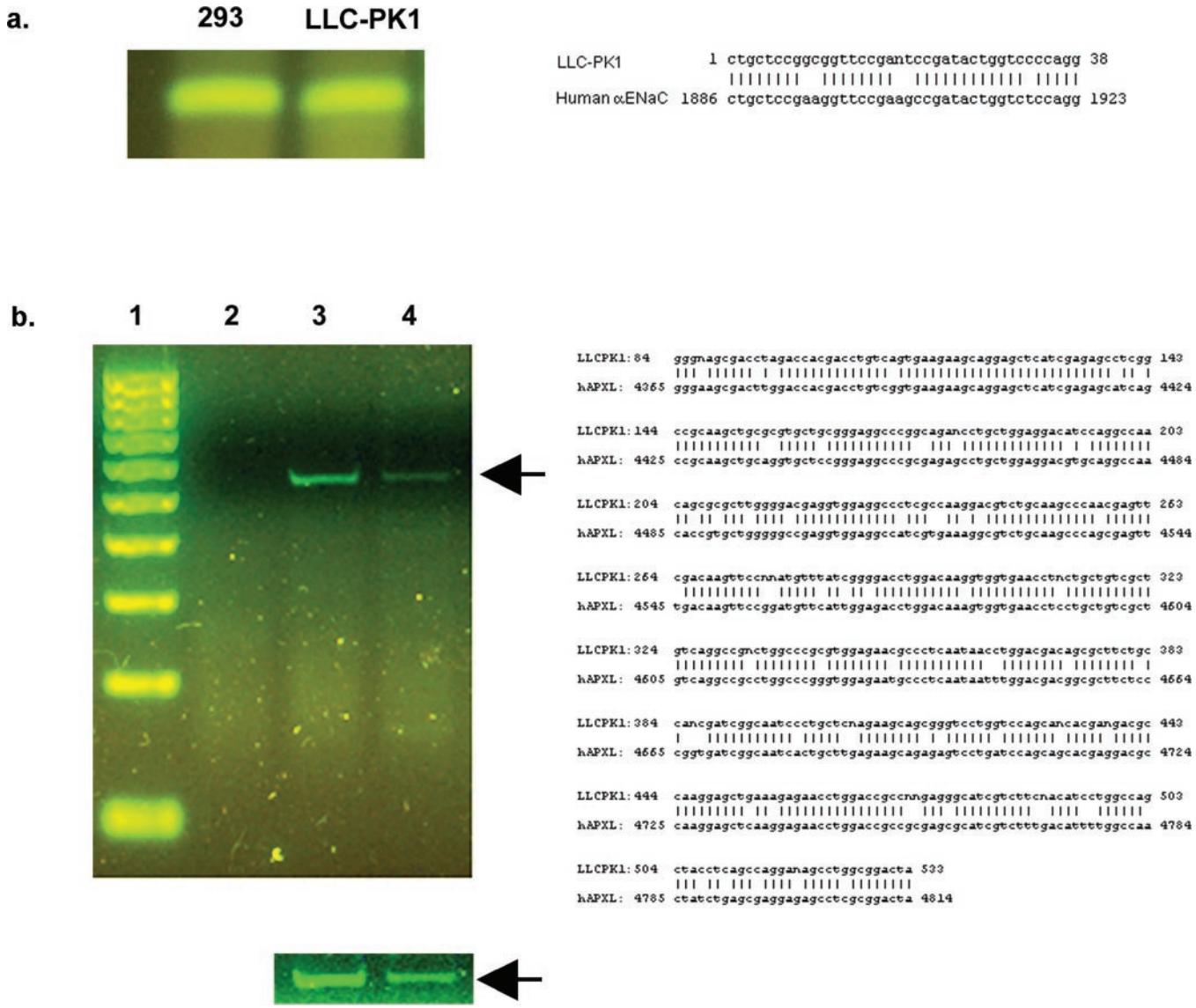

FIG. 4. **RT-PCR of LLC-PK1 mRNA.** *a*, the presence of αENaC in total RNA from LLC-PK1 cells was determined by RT-PCR (Left) with primers selective for the α subunit of bovine ENaC (16). Positive control was conducted with mRNA from human 293 embryonic kidney cells. PCR products were separated on 3% agarose gel, indicating the 105-bp expected band. *Right panel*, sequence comparison of the RT-PCR product from LLC-PK1 and human αENaC, indicating very high homology. *b*, *left panel*, the presence of ApxL in total RNA from LLC-PK1 cells was determined with primers selective for the human homolog of Apx (ApxL, as originally reported (15)). *Lane 1*, nucleotide ladder; *lane 2*, negative control; *lane 3*, LLC-PK1 RT-PCR material; *lane 4*, RT-PCR material from A6 cells. The amplified products of RNA isolated from LLC-PK1 and A6 cells is further shown in the *bottom panel*, indicating that the ApxL primers effectively recognized amphibian Apx. The *arrow* indicates the predicted 575-bp band. *Right panel*, nucleotide sequence comparison of LLC-PK1 RT-PCR product with human ApxL. High homology is observed.

served (Fig. 7), which were specific for either protein, including 90, 155, and 178 kDa for αENaC labeling, and 118, 151, 178, and 220 kDa for Apx(L). These data suggest that both proteins (and/or peptides related to them) are present in the same membranes. At present, the nature of the antibodies precluded us from obtaining a co-labeling of both proteins. However, affinity-purified actin complexes co-precipitated both proteins after purification. This possible interaction with cytoskeleton-associated complexes is consistent with previous reports on Apx-ENaC complexes in A6 cells (24) and will be further explored elsewhere (data not shown).

DISCUSSION

The first step in electrodifussional Na^+ transport across distal renal epithelia entails its selective movement into the cytosol through apical cation-selective channels. Little information is available, however, about the presence and potential physiological roles of ion channels responsible for apical Na^+ channel activity in proximal tubular cells. As much as 10% of the apical Na^+ conductance in the proximal nephron may be accounted for by electrodifussional pathways (25). However, the possibility that the mammalian proximal tubule expresses

(*right bottom panel*), showing that the open state contains a smaller subconductance state. *d*, current-voltage relationship of AVP-induced (*circles*) and PKA-induced (*triangles*) Na^+ channel activity in LLC-PK_1 cells. AVP data were obtained after excision of AVP-treated cells under cell-attached conditions and direct addition of PKA and ATP under excised conditions. Both single channel conductances were identical, although higher dispersion is observed for the AVP-treated data. This is suggestive of frequent presence of subconductance states. The data are the means ± S.E. from 13 and 17 experiments for AVP and PKA treated cells, respectively. *e*, Na^+ channel activity obtained either under spontaneous conditions (*top tracing*) and/or AVP treatment was completely inhibited by the addition of activated pertussis toxin (100 ng/ml, *middle tracing*). This effect was rapidly reversed after the addition of GTPγS (1 mM, *bottom tracing*). The data are representative of four experiments.

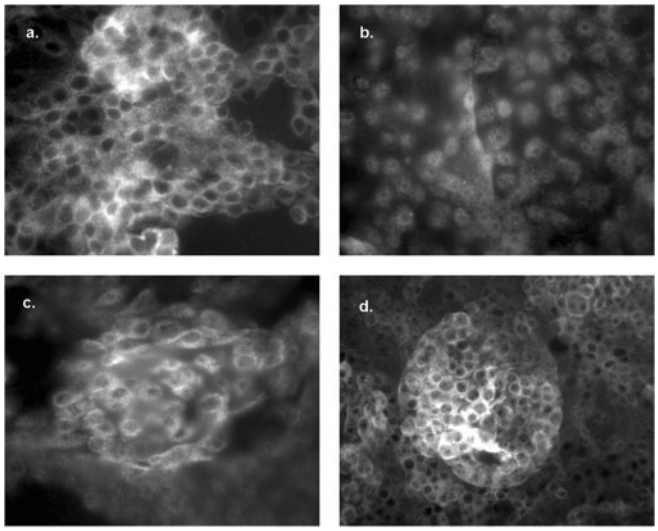

FIG. 5. **Immunocytochemical labeling of αENaC in LLC-PK1 cells.** *a*, subconfluent monolayers of LLC-PK1 cells were immunolabeled with the anti-αENaC antibody. The αENaC labeling was largely intracellular. Images were observed at 20×. *b*, nonspecific labeling was observed, however, in the presence of αENaC immunogenic peptide (15 μg/ml). *c*, αENaC labeling was also observed in domes of fluid transporting cells. *d*, αENaC immunolabeling was not modified by the presence of AVP (10 μM). The data are representative of two or three experiments under each condition.

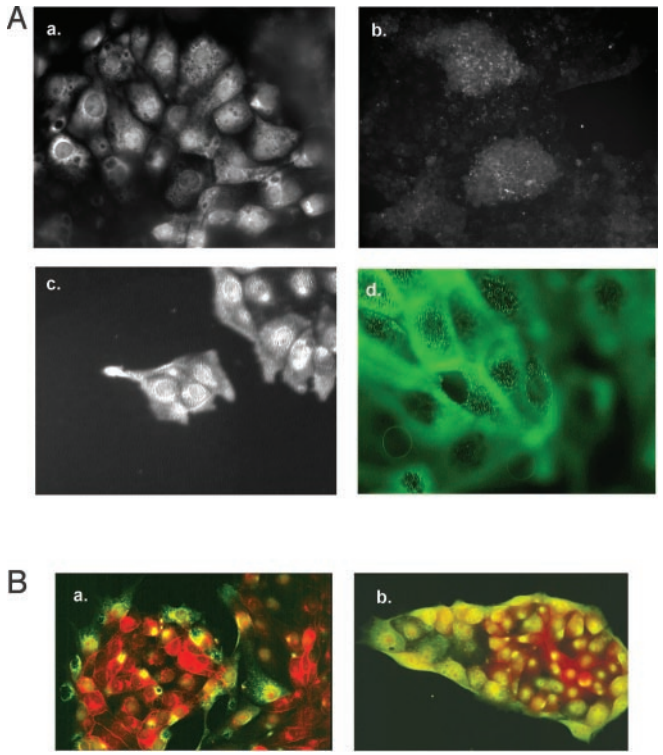

FIG. 6. **Immunocytochemical labeling of ApxL in LLC-PK1 cells.** *A*, *a*, subconfluent monolayers of LLC-PK1 cells were immunolabeled with anti-Apx antibody (FITC, *green*) and Evans Blue to counterstain for cellular morphology. *b*, labeling in the presence of immunogenic peptide (15 μg/ml) indicated low nonspecific immunoreactivity. The images were obtained at 40×. *c*, strongest ApxL labeling was observed in peripheral cells. *d*, Apical ApxL was clearly observed (X60). *B*, *a*, ApxL labeling of control, subconfluent cell islands was stronger in peripheral and weaker in internal cells. *b*, dramatic Apx redistribution was observed after treatment with AVP (10 μM). AVP-treated cells displayed an increase in both apical and intracellular ApxL staining. The images were observed at 40×. The data are representative of at least three experiments.

Na^+-permeable cation channels is a still an open question. Early evidence suggested the presence of Na^+ channels in brush border membranes of the renal proximal tubule. This includes NMR measurements of rapid Na^+ exchange (26) and the hyperpolarizing effect of amiloride on the apical membrane of mouse straight proximal tubules (27). More direct evidence for the presence of amiloride-sensitive Na^+ channels (12 pS) has been provided by patch-clamp studies of apical membranes from rabbit late (*pars recta*) (28) and rat (29) proximal tubules. The molecular nature of Na^+-permeable cation channels in proximal tubule preparations is still unknown. A cGMP-gated, amiloride-sensitive, nonselective, 28-pS channel has been reported in proximal tubules (30). Further, Willmann *et al.* (29) demonstrated the presence of an amiloride-sensitive Na^+-permeable conductance in rat proximal tubules. In that study, the presence of α, β, and γ-ENaC message was determined. The single channel conductance and the actual involvement of ENaC subunits in this Na^+ conductance, however, were not assessed. The consensus and previous evidence would indicate that the mammalian proximal convoluted tubule does not express a functional ENaC channel (31–33).

LLC-PK1 cells are a useful *in vitro* renal tubular epithelial cell model with several properties of the *pars recta* of the proximal tubule (1). Several Na^+ transport mechanisms have been previously described in LLC-PK1 cells (2, 3). Earlier studies from our laboratory determined the presence of electrodiffusional Na^+ transport in LLC-PK1 cells (7). Based on its contribution to the resting membrane potential, its high affinity for amiloride, and blockage by extracellular La^{3+} (7), this Na^+ pathway was deemed consistent with the possible presence of Na^+-permeable channels in these cells. At least one earlier preliminary patch-clamping study supported this contention (10).

To investigate whether Na^+-permeable channels are present in LLC-PK1 cells, in the present study we applied patch-clamping techniques to these cells. Single channel currents were observed in cell-attached and excised, inside-out patches of LLC-PK1 cells. Spontaneous Na^+-selective channel currents displayed an 11-pS single channel conductance and a 3:1 Na^+/K^+ permeability-selectivity ratio. AVP under cell-attached conditions and PKA and ATP under excised conditions activated the Na^+-permeable channels in LLC-PK1 cells. Both spontaneous and cAMP-activated single channel currents in LLC-PK1 cells were similar to the 9-pS Na^+ channels previously observed in A6 renal epithelial cells (11, 17–19). However, depending on the activation process, channels showed different kinetics (Figs. 1*a* and 2) and frequent subconductance states of 8 and 3 pS, respectively. Similar findings were observed by channel reconstitution of LLC-PK1 cell membranes in a lipid bilayer, although the single channel conductance was slightly higher under these conditions. This channel activity is consistent with the expression of Apx but not ENaC in A6 renal epithelial cells.

The molecular identity of the Na^+ channels present in LLC-PK1 cells will require further experimentation. Nevertheless, inhibition by activated PTX (Fig. 2) and reversal by GTPγS are both consistent with previous evidence of G protein regulation of Apx (17). The highly selective, 4-pS, amiloride blockable Na^+ channel (the Na^+/K^+ permeability-selectivity ratio > 30), expected to be the ENaC phenotype in A6 cells, in contrast, is actually activated by PTX and inhibited by GTP analogs (22). This channel phenotype is not activated by cholera toxin (22), a maneuver mimicking the AVP response in LLC-PK1 cells, which increased surface labeling of ApxL but not ENaC in LLC-PK1 domes.

To initiate a characterization of membrane proteins potentially associated with the Na^+ channel activity of LLC-PK1

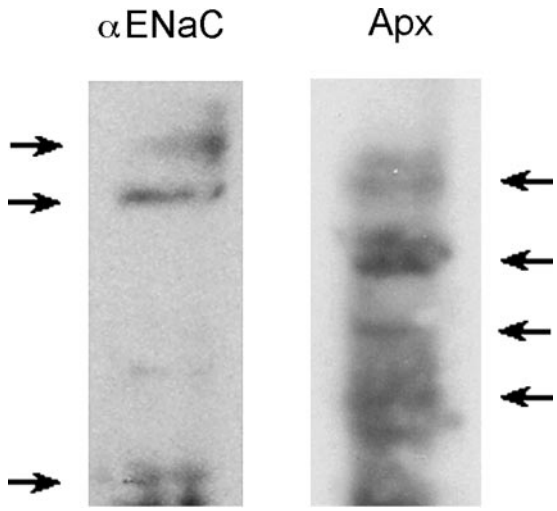

FIG. 7. **Western blot analysis of ApxL and αENaC in LLC-PK1 plasma membranes.** The cell membranes from LLC-PK1 cells were obtained according to procedures previously described (12), and the membranes were separated by 4–12% SDS-PAGE and electroblotted into polyvinylidene difluoride membrane. The blots were immunoblotted with anti-αENaC (*left panel*) and anti-Apx (*right panel*) antibodies separately (both antibodies were a kind gift of Dr. Tom Kleyman). Nonspecific labeling was competed with specific immunogenic peptides (data not shown). The data are representative of two preparations.

cells, RT-PCR analysis was conducted in mRNA from these cells. LLC-PK1 subconfluent monolayers expressed porcine orthologs of αENaC and ApxL, the human homolog of Apx (15). A molecular complex containing both Apx and αENaC has been observed in A6 epithelial cells (24), suggesting that the two proteins may be associated and functionally implicated in yet to be characterized channel complexes. Nevertheless, the presence of a functional ENaC in proximal tubule preparations is still a matter of debate. Duc *et al.* (31) were unable to detect ENaC in the mammalian proximal tubule. Greger's group, however, reported an amiloride-sensitive change in transepithelial potential and mRNA for α, β, and γ-ENaC subunits in rat proximal tubules (29). The evidence in this report does not unequivocally ascribe either ENaC subunits or Apx(L) proteins to the Na^+ channel complex in LLC-PK1 cells but rather provide preliminary evidence to indicate that one of these proteins alone, in a complex, or in association with yet to be identified membrane proteins may be responsible for this channel activity as in other cells. It is also important to note that LLC-PK1 cells express V2 vasopressin receptors, and a robust cAMP stimulatory response is not expected in proximal convoluted tubules of the mammalian nephron. Because the proximal tubular transport properties of the porcine kidney are still largely unknown, further investigations will be required to identify the various contributors to this channel activity. Full cloning and sequencing of the proteins described in this report are required before other proteins are assessed, including ENaC isoforms.

The presence and vasopressin-induced redistribution of Apx(L) in LLC-PK1 cells is of particular interest, because the channel properties and regulation are most consistent with Apx-associated channel activity. Apx is a 120–170-kDa protein (23) associated with the apical epithelial Na^+ channel complex originally purified by Benos and collaborators (34). The 150-kDa subunit of the A6 Na^+ channel complex displays channel activity in lipid bilayers (35). Thus, Apx and the 150-kDa subunit may represent the same transmembrane protein, and the possibility was originally raised that Apx may be the pore-bearing component of a renal epithelial Na^+ channel. The original study failed to detect amiloride-sensitive Na^+ channel activity after Apx expression in *Xenopus* oocytes (23). However, studies from our laboratory (12) demonstrated that expression of Apx in ABP-280-deficient human melanoma cells is associated with 9-pS Na^+ channel activity, similar to that reported in the present study. This channel is also functionally similar to the 9-pS apical Na^+ channel of A6 cells (11, 17–19, 36). Apx-mediated Na^+-permeable ion channel currents are regulated both by PKA and actin (12). Thus, the AVP and PKA regulation of the 11-pS Na^+ channel in LLC-PK1 cells share similarities with the 9-pS Na^+ channels observed in A6 amphibian epithelial cells (11, 19, 37). Although Apx is an amphibian protein, a mammalian homolog of the *Apx* gene, ApxL, has been cloned from human retina, which was also detected in brain, placenta, lung, pancreas, and kidney (15). The *Apxl* gene encodes a 1616-amino acid protein sharing significant sequence homology with Apx. The sequence homology of the LLC-PK1 gene product indicates the presence of a porcine ortholog of ApxL. It is important to indicate, however, that ApxL channel function is not demonstrated in this study. Further investigation will be required to assess whether the sequence homology between the amphibian Apx and the porcine ortholog of ApxL extend to their functional properties.

Because of the presence of both αENaC and ApxL gene products in LLC-PK1 cells, the possibility exists for the Na^+ channel observed to be a reflection of either one of these channel proteins and/or a complex including both proteins. Several peptides of putative similarity with both ENaC and ApxL were co-expressed in LLC-PK1 membranes. This is in agreement with studies by Smith and co-workers (24), who determined the presence of a cytoskeletal complex associated with both ENaC and Apx in A6 renal epithelial cells. In conclusion, the present data determined the presence of an amiloride-sensitive 11-pS Na^+-permeable cation channel in LLC-PK1 cells. Potential limitations arise from studies on cultured cell lines as it pertains to extrapolations to *in vivo* tissues and the kidney. Nevertheless, the presence of Na^+-permeable channels in LLC-PK1 cells may be relevant for a better understanding of Na^+ reabsorption in the mammalian proximal nephron previously thought to be devoid of Na^+-permeable channels.

Acknowledgments—We thank Valeria C. Primo and Gayle Hawthorn for technical support, Dr. Tom R. Kleyman for useful discussions concerning various aspects of the manuscript, Drs. Tom R. Kleyman and Jonathan Zuckerman for providing antibodies for staining cells. We also acknowledge Dr. Marcelo D. Carattino for help conducting some of the patch-clamping experiments and Nicolás Montalbetti, Gustavo Timpanaro, and Jimena Semprine for help with the reconstitution studies.

REFERENCES

1. Hull, R. N., Cherry, W. R., and Weaver, G. W. (1976) *In Vitro Cell Dev. Biol.* **12,** 670–677
2. Rabito, C. A., and Karish, M. V. (1982) *J. Biol. Chem.* **257,** 6802–6808
3. Rabito, C. A. (1986) *Am. J. Physiol.* **250,** F734–F743
4. Rabito, C. A., and Ausiello, D. A. (1980) *J. Membr. Biol.* **54,** 31–38
5. Rabito, C. A. (1983) *Am. J. Physiol.* **245,** F22–F31
6. Cantiello, H. F., Scott, J. A., and Rabito, C. A. (1986) *J. Biol. Chem.* **261,** 3252–3258
7. Cantiello, H. F., Scott, J. A., and Rabito, C. A. (1987) *Am. J. Physiol.* **252,** F590–F597
8. Ausiello, D. A., Stow, J. L., Cantiello, H. F., de Almeida, J. B., and Benos, D. J. (1992) *J. Biol. Chem.* **267,** 4759–4765
9. Moran, A., Asher, C., Cragoe, E. J., Jr., and Garty, H. (1988) *J. Biol. Chem.* **263,** 19586–19591
10. Moran, A., and Moran, N. (1984) *Fed. Proc.* **43,** 447
11. Cantiello, H. F., Stow, J., Prat, A. G., and Ausiello, D. A. (1991) *Am. J. Physiol.* **261,** C882–C888
12. Prat, A., Holtzman, E., Brown, D., Cunningham, C., Reisin, I., Kleyman, T., McLaughlin, M., Jackson, G., Jr., Lydon, J., and Cantiello, H. (1996) *J. Biol. Chem.* **271,** 18045–18053
13. González-Perrett, S., Kim, K., Ibarra, C., Damiano, A. E., Zotta, E., Batelli, M., Harris, P. C., Reisin, I. L., Arnaout, M. A., and Cantiello, H. F. (2001) *Proc. Natl. Acad. Sci. U. S. A.* **98,** 1182–1187
14. Smith, P. R., Mackler, S. A., Weiser, P. C., Brooker, D. R., Ahn, Y. J., Harte, B. J., McNulty, K. A., and Kleyman, T. R. (1998) *Am. J. Physiol.* **274,** F91–F96
15. Schiaffino, M. V., Bassi, M. T., Rugarli, E. I., Renieri, A., Galli, L., and

Ballabio, A. (1995) *Hum. Mol. Genet.* **4,** 373–382
16. Fuller, C. M., Awayda, M. S., Arrate, M. P., Bradford, A. L., Morris, R. G., Canessa, C. M., Rossier, B. C., and Benos, D. J. (1995) *Am. J. Physiol.* **272,** C641–C654
17. Cantiello, H. F., Patenaude, C. R., and Ausiello, D. A. (1989) *J. Biol. Chem.* **264,** 20867–20870
18. Hamilton, K. L., and Eaton, D. C. (1985) *Am. J. Physiol.* **249,** C200–C207
19. Prat, A. G., Ausiello, D. A., and Cantiello, H. F. (1993) *Am. J. Physiol.* **265,** C218–C223
20. Goldring, S. R., Dayer, J. M., Ausiello, D. A., and Krane, S. M. (1978) *Biochem. Biophys. Res. Commun.* **83,** 434–440
21. Ausiello, D. A., Hall, D. H., and Dayer, J. M. (1980) *Biochem. J.* **186,** 773–780
22. Ohara, A., Matsunaga, H., and Eaton, D. C. (1993) *Am. J. Physiol.* **264,** C352–C360
23. Staub, O., Verrey, F., Kleyman, T. R., Benos, D. J., Rossier, B. C., and Kraehenbuhl, J.-P. (1992) *J. Cell Biol.* **119,** 1497–1506
24. Zuckerman, J., Chen, X., Jacobs, J., Hu, B., Kleyman, T. R., and Smith, P. R. (1999) *J. Biol. Chem.* **274,** 23286–23295
25. Weinstein, A. M. (2000) in *The Kidney: Physiology & Pathophysiology* (Seldin, D. W., and Giebish, G., eds) Vol. 3, 3rd Ed., pp. 1287–1331, Lippincott Williams & Wilkins, Philadelphia
26. Elgavish, G. A., and Elgavish, A. (1985) *Biochem. Biophys. Res. Commun.* **128,** 746–753
27. Volkl, H., and Lang, F. (1988) *Biochim. Biophys. Acta* **946,** 5–10
28. Gögelein, H., and Greger, R. (1986) *Pflugers Arch.* **406,** 198–203
29. Willmann, J. K., Bleich, M., Rizzo, M., Schmidt-Hieber, M., Ullrich, K. J., and Greger, R. (1997) *Pfluegers Arch.* **434,** 173–178
30. Ciampolillo, F., McCoy, D. E., Green, R. B., Karlson, K. H., Dagenais, A., Molday, R. S., and Stanton, B. A. (1996) *Am. J. Physiol.* **271,** C1303–C1315
31. Duc, C., Farman, N., Canessa, C., Bonvalet, J.-P., and Rossier, B. (1994) *J. Cell Biol.* **127,** 1907–1921
32. Loffing, J., Loffing-Cueni, D., Macher, A., Hebert, S. C., Olson, B., Knepper, M. A., Rossier, B. C., and Kaissling, B. (2000) *Am. J. Physiol.* **278,** F530–F539
33. Hager, H., Kwon, T. H., Vinnikova, A. K., Masilamani, S., Brooks, H. L., Frokiaer, J., Knepper, M. A., and Nielsen, S. (2001) *Am. J. Physiol.* **280,** F1093–F1106
34. Benos, D. J., Saccomani, G., Brenner, B. M., and Sariban-Sohraby, S. (1986) *Proc. Natl. Acad. Sci. U. S. A.* **83,** 8525–8529
35. Sariban-Sohraby, S., and Fisher, R. S. (1992) *Am. J. Physiol.* **263,** C1111–C1117
36. Cantiello, H. F., Patenaude, C. R., Codina, J., Birnbaumer, L., and Ausiello, D. A. (1990) *J. Biol. Chem.* **265,** 21624–21628
37. Prat, A. G., Bertorello, A. M., Ausiello, D. A., and Cantiello, H. F. (1993) *Am. J. Physiol.* **265,** C224–C233